6. SYNTHESIS OF SERIES II

6. Synthesis - Series II-Indole Thiazolidinedione hybrid analogues

6.1. Rationale

The synthesized indole-TZD hybrid analogues (Series I) exhibited a potential PL inhibition with the most active analogue from the series, **5r** that exhibited an IC_{50} value of 7.30 µM. Further molecular modelling analysis of orlistat and **5r** revealed that the latter possessed greater interaction distance between the reactive carbonyl group of imide group of TZD and Ser 152 of the active site (**Fig. 6.1**). This might be the probable reason for a lesser PL inhibitory potential.

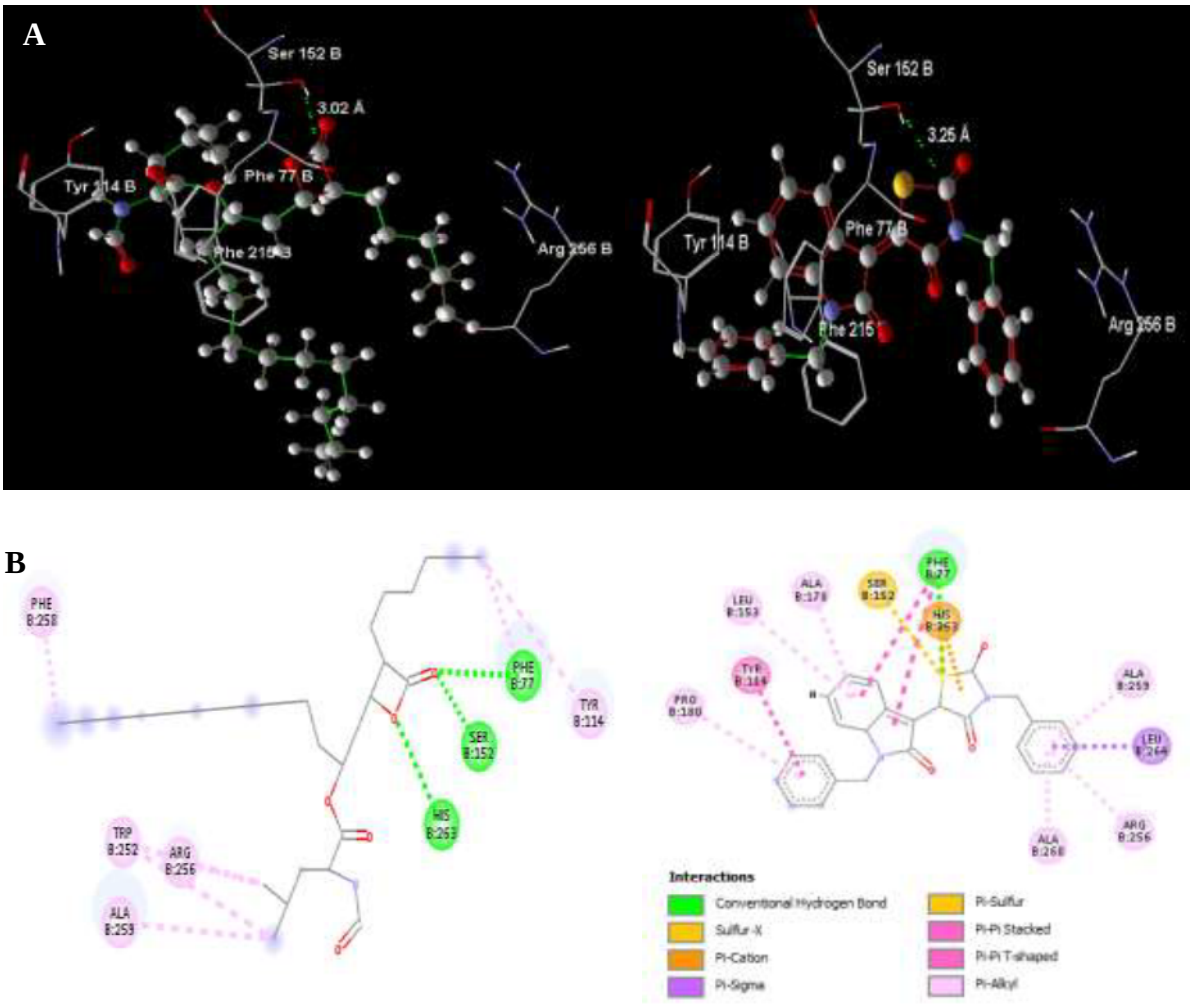

Fig. 6.1. (**A**) 3D poses of **orlistat** and **5r** highlighting the distance of reactive carbonyl from Ser152 (3.02 and 3.25 Å, respectively); (**B**) 2D interactions of orlistat and 5r

Thus, the present chapter was focussed on understanding the effect of linker groups between the indole and TZD. Preliminary molecular modelling study highlighted that the incorporation of an additional carbon atom between the indole and TZD scaffold might be helpful for the reduction of the interaction distance of the carbonyl group from Ser152

(**Fig. 6.2**) Accordingly, a series of 28 indole-TZD analogues were designed, synthesized, characterized and evaluated for their *in-vitro* PL inhibitory potential.

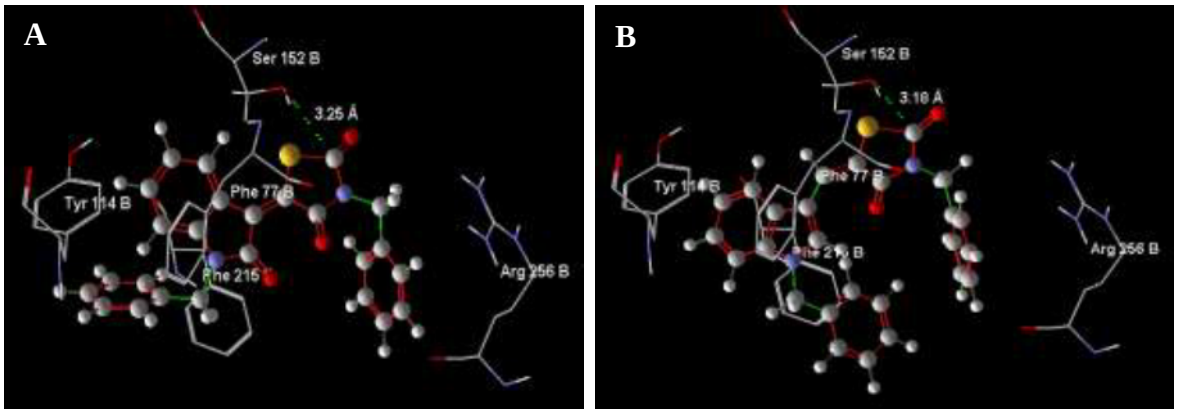

Fig. 6.2. Rationale for designing series II Indole-TZD analogues as PL inhibitors. The interaction distance has reduced from 3.25 Å in **5r** (**A**) to 3.16 Å by the incorporation of an additional carbon linker (**B**)

6.2. Synthesis and Characterization

The syntheses of all the final analogues **6a** to **6ab** were carried out as per the procedure detailed in **Scheme 6.1**. Synthesis and characterization of TZD scaffold and final analogues was performed in the same manner as discussed in the previous chapter (Chapter 5).

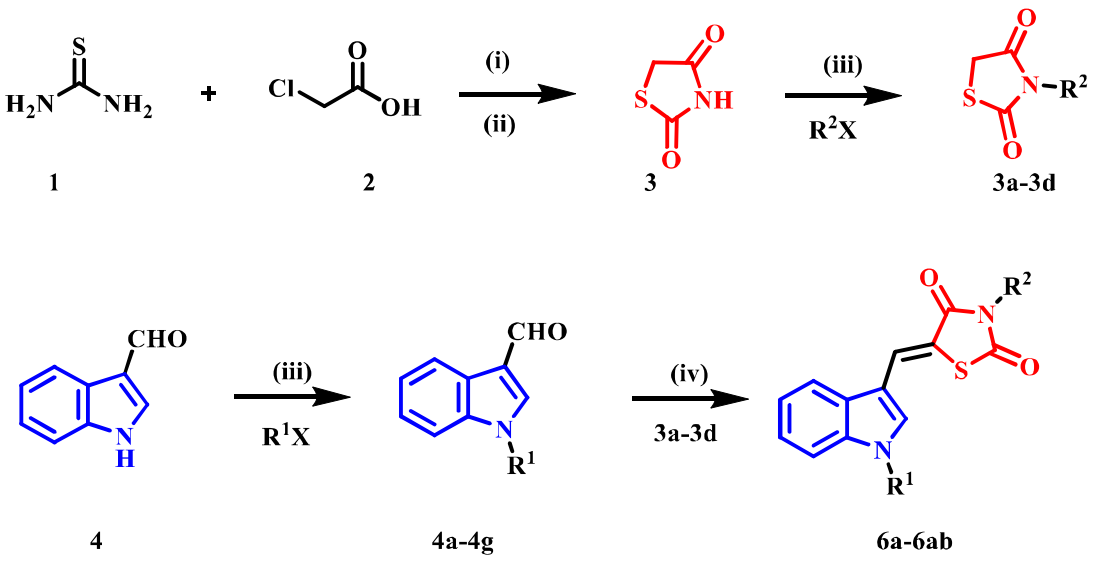

R^1- H, Methyl, Ethyl, Benzyl, *P*-chlorobenzyl, *P*-bromobenzyl , *P*-nitrobenzyl
R^2- Benzyl, *P*-chlorobenzyl, *P*-bromobenzyl, *P*-nitrobenzyl

Scheme 6.1. Synthesis of series II analogues (6a - 6ab). Reagents and conditions (i) 0-5°C, 30 min; (ii) HCl, H_2O, 110-120 °C, 10-12 h; (iii) NaH, DMF, overnight; (iv) Piperidine, glacial acetic acid, EtOH, 6-8 h, Reflux

General procedure for the synthesis of N-substituted indole-3-carbaldehyde derivatives (4a-4g)

Condensation of indole-3-carbaldehyde (**4**, 1 eq.) with various alkyl/aryl halides (1.5 eq.) was performed in the presence of NaH (1.5 eq.) in anhydrous DMF. After the specified time of stirring, the solution was poured into the ice-cold water and the obtained precipitate was filtered and recrystallized from the appropriate solvents to obtain **4a** to **4g** [1].

General procedure for the synthesis of indole-TZD hybrid analogues (6a to 6ab)

To a mixture of 1,3-thiazolidine-2,4-dione derivatives (**3a-3d**) (2mmol) and indole-3-carbaldehydes and their derivatives (**4, 4a-ag**) (2 mmol) in ethanol, few drops of piperidine and glacial acetic acid was added and the reaction mixture was refluxed. A solid was separated out of the reaction mixture within 1 h and the refluxing was continued for 6-8 h to complete the reaction. The reaction mixture was cooled to room temperature and the obtained solids were filtered [2,3]. The analogues (**6a-6ab**) were purified by column chromatography or recrystallization with ethanol.

Characterisation

The reaction of various indole carboxaldehyde derivatives with TZD primarily involves the Knoevenagel condensation. The analogues (**6a-6ab**) were obtained in good yield with a buff yellowish colour and were characterized by ATIR, ^{1}H, ^{13}C NMR spectroscopy and mass spectrometry HRMS [ESI mode]. The obtained data were in good agreement with their structural identity. The IR spectrum of the analogues (**6a-6ab**) showed strong absorption bands at 1697-1746 and 1653-1699 cm^{-1} due to two carbonyl groups. The disappearance of methylene proton (3.95 δ ppm) of TZD and appearance of arylidene (=CH-) peak further confirmed the formation of the hybrid analogues. Arylidene proton in the target analogues can exist as "*E*" and "*Z*" configuration. Yu Momose *et al*., revealed that the arylidene proton in "*Z*" configuration will resonate at 7.4 to 8.2 δ ppm, while the "*E*" configuration resonates at 6.2 to 6.8 δ ppm. Anisotropic effect of TZD carbonyl group resulted in the desheilding of arylidene proton. Further, due to the intramolecular hydrogen bond between the TZD carbonyl group and arylidene proton, formation of thermodynamically stable "*Z*" configuration [2–4] is favoured. In the present work, arylidene groups proton appeared as singlet or multiplet at >8.26 δ ppm, indicating that the analogues predominantly formed were in "*Z*" configuration. All other protons were

observed in expected regions. The appearance of three C=O peaks in ^{13}C NMR (165 to 173 δ ppm) further confirmed the condensation of TZD and indole scaffolds. All the analogues showed a prominent signal at δ 15-51 due to the presence of various alkyl groups. Finally, the assigned structures of various analogues were confirmed by their mass spectra where characteristic $[M+H]^+$ peaks were observed. Detailed information on characterisation of all the analogues are given below.

(Z)-5-((1H-Indol-3-yl)methylene)-3-benzylthiazolidine-2,4-dione (6a)

Yield: 48%; Buff yellow solid; m.p: 243-244 °C; ^1H NMR (400 MHz, $CDCl_3$) δ 8.29 (s, 1H,-H of methylene), 7.86 (d, *J* = 7.6 Hz, 1H, H_7 of indole), 7.55 (d, *J* = 2.8 Hz, 1H, H_4 of indole), 7.50 – 7.45 (m, 3H, aromatic), 7.39 – 7.30 (m, 5H, aromatic), 4.94 (s, 2H, $-CH_2$); ^{13}C NMR (100 MHz, $CDCl_3$) δ 167.50, 166.19, 135.78, 135.47, 128.83, 128.71, 128.13, 127.05, 126.79, 125.96, 124.04, 121.89, 118.79, 115.96, 112.47, 111.70, 45.21; IR (ATR) υ; 3258, 2923, 2855, 2330, 1716, 1658, 1589, 1508, 1457, 1423, 1375, 1317, 1217, 1140, 1103, 967, 820, 736, 695, 662 cm^{-1}; HRMS (ESI^+) calculated for $C_{19}H_{14}N_2O_2S$ $[M+H]^+$, 335.0854; found 335.0795.

(Z)-3-Benzyl-5-((1-methyl-1H-indol-3-yl)methylene)thiazolidine-2,4-dione (6b)

Yield: 65%; Buff yellow solid; m.p: 223-224°C; ^1H NMR (400 MHz, $CDCl_3$) δ 8.26 (s, 1H,-H of methylene), 7.85 (dd, *J* = 7.7, 1.2 Hz, 1H, H_7 of indole), 7.53 – 7.45 (m, 2H, aromatic), 7.45 – 7.27 (m, 7H, aromatic), 4.93 (s, 2H, $-CH_2$), 3.90 (s, 3H, $-CH_3$); ^{13}C NMR (100 MHz, $CDCl_3$) δ 167.51, 166.22, 136.96, 135.58, 131.23, 128.86, 128.69, 128.10, 127.91, 125.87, 123.66, 121.74, 118.86, 114.56, 110.93, 110.00, 45.17, 33.71; IR (ATR) υ; 3856, 3740, 3613, 2364, 1717, 1663, 1592, 1521, 1464, 1363, 1320, 1237, 1134, 1060, 1014, 965, 833, 732, 695, 652 cm^{-1}; HRMS (ESI^+) calculated for $C_{20}H_{16}N_2O_2S$ $[M+H]^+$, 349.1011; found 349.1005.

(Z)-3-Benzyl-5-((1-ethyl-1H-indol-3-yl)methylene)thiazolidine-2,4-dione (6c)

Yield: 60%; Buff yellow solid; m.p: 177 -178 °C; ^1H NMR (400 MHz, $CDCl_3$) δ 8.27 (s, 1H, -H of methylene), 7.85 (m, 1H, , aromatic), 7.53 – 7.47 (m, 2H, aromatic), 7.44 – 7.26 (m, 7H, aromatic), 4.93 (s, 2H, $-CH_2$), 4.27 (q, *J* = 7.3 Hz, 2H, $-CH_2$ of ethyl), 1.56 (t, *J* = 7.3 Hz, 3H, $-CH_3$ of ethyl); ^{13}C NMR (100 MHz, $CDCl_3$) δ 167.51, 166.22, 136.05, 135.61, 129.60, 128.83, 128.69, 128.14, 128.08, 125.95, 123.54, 121.70, 118.99, 114.43, 111.05, 110.10, 45.17, 41.97, 15.19; IR (ATR) υ; 3852, 3742, 3673, 3613, 2363, 2319, 1661, 1520,

1467, 1364, 1324, 1219, 1137, 1067, 970, 832, 735, 656 cm^{-1}; HRMS (ESI^+) calculated for $C_{21}H_{18}N_2O_2S$ $[M+H]^+$, 363.1167; found 363.1150.

(Z)-3-Benzyl-5-((1-benzyl-1H-indol-3-yl)methylene)thiazolidine-2,4-dione (6d)

Yield: 63%; Buff yellow solid; m.p: 188-189 °C; ^1H NMR (400 MHz, $CDCl_3$) δ 8.27 (s, 1H, -H of methylene), 7.87 (dd, *J* = 6.9, 2.1 Hz, 1H, H_7 of indole), 7.51 – 7.40 (m, 3H, aromatic), 7.40 – 7.24 (m, 9H, aromatic), 7.15 – 7.03 (m, 2H, aromatic), 5.38 (s, 2H, -CH_2), 4.93 (s, 2H, -CH_2); ^{13}C NMR (100 MHz, $CDCl_3$) δ 167.47, 166.19, 136.55, 135.63, 135.54, 130.55, 129.09, 128.81, 128.69, 128.30, 128.14, 128.10, 126.98, 125.76, 123.81, 121.89, 119.00, 115.16, 111.49, 110.57, 51.00, 45.18; IR (ATR) υ; 3852, 3742, 3673, 3613, 3222, 3111, 2360, 2323, 1673, 1520, 1465, 1374, 1190, 1143, 1094, 1025, 974, 794, 736, 700 cm^{-1} ; HRMS (ESI^+) calculated for $C_{26}H_{20}N_2O_2S$ $[M+H]^+$, 425.1324; found 425.1302.

(Z)-3-Benzyl-5-((1-(4-chlorobenzyl)-1H-indol-3-yl)methylene)thiazolidine-2,4-dione (6e)

Yield: 65%; Buff yellow solid; m.p: 208-209 °C; ^1H NMR (400 MHz, $CDCl_3$) δ 8.27 (s, 1H, -H of methylene), 7.87 (dd, *J* = 6.9, 2.1 Hz, 1H, H_7 of indole), 7.51 – 7.40 (m, 3H,aromatic), 7.40 – 7.24 (m, 9H, aromatic), 7.15 – 7.03 (m, 2H, aromatic), 5.38 (s, 2H, -CH_2), 4.93 (s, 2H, -CH_2). ^{13}C NMR (100 MHz, $CDCl_3$) δ 167.35, 166.15, 136.36, 135.49, 134.21, 134.20, 130.31, 129.28, 128.82, 128.70, 128.18, 128.15, 128.13, 125.56, 123.96, 122.00, 119.10, 115.53, 111.73, 110.45, 50.37, 45.21; IR (ATR) υ; 3841, 3747, 3672, 3613, 3567, 3011, 2874, 2656, 2464, 2357, 1697, 1653, 1517, 1362, 1311, 1186, 1129, 805, 733, 686 cm^{-1}; HRMS (ESI^+) calculated for $C_{26}H_{19}ClN_2O_2S$ $[M+H]^+$, 459.0934; found 459.0925.

(Z)-3-Benzyl-5-((1-(4-bromobenzyl)-1H-indol-3-yl)methylene)thiazolidine-2,4-dione (6f)

Yield: 53%; Buff yellow solid; m.p: 216-217 °C; ^1H NMR (400 MHz, $CDCl_3$) δ 8.27 (s, 1H, -H of methylene), 7.87 (ddd, *J* = 7.0, 3.4, 2.1 Hz, 1H, H_7 of indole), 7.51 – 7.42 (m, 5H,aromatic), 7.41 – 7.27 (m, 6H,aromatic), 7.07 – 6.97 (m, 2H,aromatic), 5.37 (s, 2H, -CH_2), 4.93 (s, 2H, -CH_2); ^{13}C NMR (100 MHz, $CDCl_3$) δ 167.34, 166.15, 136.35, 135.49, 134.75, 132.24, 130.30, 128.82, 128.70, 128.50, 128.46, 128.17, 128.13, 125.54, 123.97, 122.01, 119.11, 115.57, 111.75, 110.44, 50.42, 45.21; IR (ATR) υ; 3852, 3742, 3673, 3613, 2799, 2361, 2324, 1917, 1745, 1697, 1652, 1520, 1316, 1187, 1128, 1009, 918, 796,

735, 690 cm^{-1}; HRMS (ESI^+) calculated for $C_{26}H_{19}BrN_2O_2S$ $[M+H]^+$, 503.0429; found 503.0417.

(Z)-3-Benzyl-5-((1-(4-nitrobenzyl)-1H-indol-3-yl)methylene)thiazolidine-2,4-dione (6g)

Yield: 51%; Buff yellow solid; m.p: 198-201 °C; ^1H NMR (400 MHz, $CDCl_3$) δ 8.28 (s, 1H, -H of methylene), 8.21 (d, *J* = 8.7 Hz, 2H, H_7 of indole), 7.94 – 7.86 (m, 1H,aromatic), 7.48 (d, *J* = 6.8 Hz, 3H, H_4 of indole), 7.40 – 7.30 (m, 6H,aromatic), 7.27 – 7.20 (m, 2H,aromatic,), 5.54 (s, 2H, $-CH_2$), 4.94 (s, 2H, $-CH_2$); ^{13}C NMR (100 MHz, $CDCl_3$) δ 167.17, 166.09, 147.81, 143.06, 136.23, 135.42, 130.10, 128.83, 128.74, 128.72, 128.18, 127.34, 125.23, 124.35, 124.27, 122.24, 119.32, 116.22, 112.24, 110.20, 50.28, 45.27; IR (ATR) υ; 3897, 3847, 3741, 3650, 3608, 2356, 1724, 1667, 1605, 1519, 1466, 1382, 1336, 1229, 1144, 1018, 852, 732, 702 cm^{-1}; HRMS (ESI^+) calculated for $C_{26}H_{19}N_3O_4S$ $[M+H]^+$, 470.1175; found 470.1177.

(Z)-5-((1H-Indol-3-yl)methylene)-3-(4-chlorobenzyl)thiazolidine-2,4-dione (6h)

Yield: 43%; Buff yellow solid; m.p: 255-256 °C; ^1H NMR (400 MHz, DMSO-d_6) δ 12.24 (s, 1H, -H of NH), 8.23 (s, 1H, -H of methylene), 7.92 (d, *J* = 7.8 Hz, 1H, H_7 of indole), 7.83 (s, 1H, H_2 of indole), 7.53 (d, *J* = 8.0 Hz, 1H, H_4 of indole), 7.43 (d, *J* = 8.1 Hz, 2H, aromatic), 7.36 (d, *J* = 8.2 Hz, 2H, aromatic), 7.24 (dt, *J* = 22.9, 7.6 Hz, 2H, aromatic), 4.84 (s, 2H,$-CH_2$); ^{13}C NMR (100 MHz, DMSO-d_6) δ 172.32, 170.57, 141.46, 140.04, 137.61, 134.80, 133.85, 132.00, 131.58, 131.48, 128.41, 126.45, 123.62, 118.57, 117.69, 115.65, 49.02; IR (ATR) υ; 3246, 3113, 2924, 2359, 1713, 1658, 1588, 1486, 1424, 1375, 1320, 1216, 1140, 1092, 1005, 964, 836, 800, 724, 671 cm^{-1}; HRMS (ESI^+) calculated for $C_{19}H_{13}ClN_2O_2S$ $[M+H]^+$, 369.0465; found 369.0402.

(Z)-3-(4-Chlorobenzyl)-5-((1-methyl-1H-indol-3-yl)methylene)thiazolidine-2,4-dione (6i)

Yield: 56%; Buff yellow solid; m.p: 221-222 °C; ^1H NMR (400 MHz, $CDCl_3$) δ 8.26 (s, 1H, -H of methylene), 7.85 (d, *J* = 7.8 Hz, 1H, H_7 of indole), 7.43 (d, *J* = 8.3 Hz, 2H, aromatic), 7.40 – 7.29 (m, 6H, aromatic), 4.88 (s, 2H, $-CH_2$), 3.91 (s, 3H, $-CH_3$); ^{13}C NMR (100 MHz, $CDCl_3$) δ 167.48, 166.10, 136.98, 134.11, 134.02, 131.32, 130.37, 128.87, 127.90, 126.16, 123.72, 121.81, 118.85, 114.28, 110.90, 110.03, 44.43, 33.75; IR (ATR) υ; 3854, 3742, 3673, 3613, 2362, 2316, 1700, 1655, 1520, 1466, 1369, 1316, 1218, 1095, 1051, 924, 801, 739, 645 cm^{-1}; HRMS (ESI^+) calculated for $C_{20}H_{15}ClN_2O_2S$ $[M+H]^+$, 383.0621; found 383.0617.

(Z)-3-(4-Chlorobenzyl)-5-((1-ethyl-1H-indol-3-yl)methylene)thiazolidine-2,4-dione (6j)

Yield: 53%; Buff yellow solid; m.p: 206-207 °C; 1H NMR (400 MHz, $CDCl_3$) δ 8.27 (s, 1H, -H of methylene), 7.86 (d, *J* = 7.8 Hz, 1H, H_7 of indole), 7.45 – 7.29 (m, 8H, aromatic), 4.89 (s, 2H), 4.28 (q, J = 7.3 Hz, 2H, $-CH_2$), 1.57 (t, J = 7.3 Hz, 3H, $-CH_3$); ^{13}C NMR (100 MHz, $CDCl_3$) δ 167.49, 166.11, 136.05, 134.09, 134.05, 130.34, 129.08, 128.87, 128.12, 126.27, 123.60, 121.77, 118.98, 114.12, 111.01, 110.14, 44.43, 42.02, 15.21; IR (ATR) υ; 3852, 3742, 3673, 3614, 2927, 2361, 2321, 1666, 1589, 1520, 1472, 1367, 1327, 1219, 1138, 1089, 838, 803, 737, 650 cm^{-1}; HRMS (ESI^+) calculated for $C_{21}H_{17}ClN_2O_2S$ $[M+H]^+$, 397.0778; found 397.0767.

(Z)-5-((1-Benzyl-1H-indol-3-yl)methylene)-3-(4-chlorobenzyl)thiazolidine-2,4-dione (6k)

Yield: 58%; Buff yellow solid; m.p: 244-244 °C; ^1H NMR (400 MHz, $CDCl_3$) δ 8.28 (s, 1H, -H of methylene), 7.91 – 7.83 (m, 1H, aromatic), 7.48 – 7.39 (m, 3H, aromatic), 7.39 – 7.29 (m, 8H, aromatic), 7.18 (dd, *J* = 7.4, 2.0 Hz, 2H, aromatic), 5.42 (s, 2H, $-CH_2$), 4.89 (s, 2H, $-CH_2$); ^{13}C NMR (100 MHz, $CDCl_3$) δ 167.43, 166.07, 136.56, 135.57, 134.11, 133.98, 130.63, 130.32, 129.09, 128.87, 128.32, 128.11, 126.97, 126.07, 123.87, 121.95, 118.98, 114.87, 111.46, 110.59, 51.03, 44.44; IR (ATR) υ; 3852, 3742, 3673, 3613, 2360, 2323, 1917, 1671, 1520, 1471, 1370, 1330, 1248, 1189, 1143, 1096, 1020, 974, 799, 736 cm^{-1}; HRMS (ESI^+) calculated for $C_{26}H_{19}ClN_2O_2S$ $[M+H]^+$, 459.0934; found 459.0854.

(Z)-3-(4-Chlorobenzyl)-5-((1-(4-chlorobenzyl)-1H-indol-3-yl)methylene)thiazolidine-2,4-dione (6l)

Yield: 55%; Buff yellow solid; m.p: 220-221 °C; ^1H NMR (400 MHz, $CDCl_3$) δ 8.27 (s, 1H, -H of methylene), 7.87 (dd, *J* = 6.2, 2.8 Hz, 1H, H_7 of indole), 7.42 (d, *J* = 8.3 Hz, 3H, aromatic), 7.38 – 7.27 (m, 7H, aromatic), 7.09 (d, *J* = 8.3 Hz, 2H, aromatic), 5.39 (s, 2H, $-CH_2$), 4.89 (s, 2H, $-CH_2$); ^{13}C NMR (100 MHz, $CDCl_3$) δ 167.31, 166.03, 136.37, 134.23, 134.15, 133.94, 130.38, 130.33, 129.29, 128.88, 128.18, 128.12, 125.85, 124.01, 122.06, 119.09, 115.25, 111.70, 110.47, 99.99, 50.39, 44.47; IR (ATR) υ; 3818, 3749, 3680, 3604, 2715, 2356, 1716, 1662, 1590, 1513, 1319, 1184, 1140, 1094, 1015, 973, 930, 805, 736, 665 cm^{-1}; HRMS (ESI^+) calculated for $C_{26}H_{18}Cl2N_2O_2S$ $[M+H]^+$, 493.0544; found 493.0459.

(Z)-5-((1-(4-Bromobenzyl)-1H-indol-3-yl)methylene)-3-(4-chlorobenzyl)thiazolidine-2,4-dione (6m)

Yield: 51%; Buff yellow solid; m.p: 230-231 °C; ^{1}H NMR (400 MHz, $CDCl_3$) δ 8.27 (s, 1H, -H of methylene), 7.87 (dt, *J* = 7.4, 3.1 Hz, 1H, H_7 of indole), 7.45 (dd, *J* = 23.7, 8.1 Hz, 5H, aromatic), 7.36 – 7.29 (m, 5H, aromatic), 7.03 (d, *J* = 8.1 Hz, 2H, aromatic), 5.37 (s, 2H, -CH_2), 4.89 (s, 2H, -CH_2); ^{13}C NMR (100 MHz, $CDCl_3$) δ 167.30, 166.03, 136.37, 134.69, 134.15, 133.94, 132.25, 130.37, 130.33, 128.88, 128.46, 128.12, 125.84, 124.03, 122.28, 122.07, 119.10, 112.42, 111.72, 110.46, 50.45, 44.48; IR (ATR) υ; 3838, 3783, 3583, 2332, 1720, 1657, 1606, 1524, 1476, 1369, 1324, 1230, 1145, 1089, 1011, 964, 835, 801, 729, 661 cm^{-1}; HRMS (ESI^+) calculated for $C_{26}H_{18}BrClN_2O_2S$ $[M+H]^+$, 537.0039; found 536.9962.

(Z)-3-(4-Chlorobenzyl)-5-((1-(4-nitrobenzyl)-1H-indol-3-yl)methylene)thiazolidine-2,4-dione (6n)

Yield: 48%; Buff yellow solid; m.p: 215-217 °C; ^{1}H NMR (400 MHz, $CDCl_3$) δ 7.70 – 7.59 (m, 4H, aromatic), 7.45 – 7.40 (m, 1H, aromatic), 7.00 – 6.84 (m, 5H, aromatic), 6.88 – 6.76 (m, 2H, aromatic), 6.70 (tt, *J* = 7.1, 5.6 Hz, 2H, aromatic), 5.23 (s, 2H, -CH_2), 4.28 (s, 2H, -CH_2); ^{13}C NMR (100 MHz, $CDCl_3$) δ 172.25, 170.54, 152.20, 149.97, 141.19, 139.99, 137.62, 137.42, 134.79, 133.85, 133.41, 132.78, 130.68, 129.17, 128.84, 127.01, 124.18, 119.68, 116.41, 115.66, 54.31, 49.07; IR (ATR) υ; 3794, 3702, 3639, 3504, 3054, 2636, 1716, 1661, 1603, 1518, 1430, 1351, 1197, 1141, 1092, 1018, 955, 839, 735, 689 cm^{-1}; HRMS (ESI^+) calculated for $C_{26}H_{18}ClN_3O_4S$ $[M+H]^+$, 504.0785; found 504.0699.

(Z)-5-((1H-Indol-3-yl)methylene)-3-(4-bromobenzyl)thiazolidine-2,4-dione (6o)

Yield: 51%; Buff yellow solid; m.p: 254-255 °C; ^{1}H NMR (400 MHz, DMSO-d_6) δ 12.23 (s, 1H, -NH), 8.22 (s, 1H, -H of methylene), 7.92 (d, *J* = 7.8 Hz, 1H, H_7 of indole), 7.83 (s, 1H, H_2 of indole), 7.60 – 7.48 (m, 3H, aromatic), 7.32 – 7.16 (m, 4H, aromatic), 4.81 (s, 2H,-CH_2); ^{13}C NMR (100 MHz, DMSO-d_6) δ 167.59, 165.83, 136.70, 135.68, 132.03, 130.36, 129.72, 127.23, 126.80, 123.70, 121.74, 121.38, 118.85, 113.81, 112.95, 110.89, 44.33; IR (ATR) υ; 3434, 3248, 2919, 2356, 1711, 1654, 1585, 1482, 1427, 1372, 1314, 1214, 1136, 1093, 1003, 961, 836, 795, 717, 666 cm^{-1}; HRMS (ESI^+) calculated for $C_{19}H_{13}BrN_2O_2S$ $[M+H]^+$, 412.9959; found 412.9879.

(Z)-3-(4-Bromobenzyl)-5-((1-methyl-1H-indol-3-yl)methylene)thiazolidine-2,4-dione (6p)

Yield: 63%; Buff yellow solid; m.p: 247-248 °C; ^{1}H NMR (400 MHz, $CDCl_3$) δ 8.27 (s, 1H, -H of methylene), 7.85 (dt, *J* = 7.9, 1.0 Hz, 1H, H_7 of indole), 7.51 – 7.46 (m, 2H, aromatic), 7.41 – 7.35 (m, 5H, aromatic), 7.32 (ddd, *J* = 8.0, 6.2, 2.0 Hz, 1H, aromatic),

4.88 (s, 2H,-CH_2), 3.92 (s, 3H,-CH_3); ^{13}C NMR (100 MHz, $CDCl_3$) δ 167.47, 166.09, 136.98, 134.51, 131.84, 131.32, 130.68, 127.90, 126.20, 123.72, 122.28, 121.81, 118.86, 114.27, 110.91, 110.03, 44.49, 33.76; IR (ATR) υ; 3853, 3742, 3673, 3613, 2363, 2316, 1700, 1662, 1602, 1521, 1471, 1372, 1319, 1222, 1130, 1057, 1010, 841, 797, 742 cm^{-1}; HRMS (ESI^+) calculated for $C_{20}H_{15}BrN_2O_2S$ $[M+H]^+$, 427.0116; found 427.0109.

(Z)-3-(4-Bromobenzyl)-5-((1-ethyl-1H-indol-3-yl)methylene)thiazolidine-2,4-dione (6q)

Yield: 58%; Buff yellow solid; m.p: 201-202 °C; ^{1}H NMR (400 MHz, $CDCl_3$) δ 8.27 (s, 1H, -H of methylene), 7.85 (dd, *J* = 7.6, 1.2 Hz, 1H, H_7 of indole), 7.51 – 7.46 (m, 2H, aromatic), 7.45 – 7.29 (m, 6H, aromatic), 4.87 (s, 2H,-CH_2), 4.34 – 4.23 (m, 2H,-CH_2), 1.57 (t, *J* = 7.3 Hz, 3H,-CH_3); ^{13}C NMR (100 MHz, $CDCl_3$) δ 167.49, 166.10, 136.05, 134.54, 131.83, 130.66, 129.70, 128.12, 126.29, 123.60, 122.26, 121.77, 118.98, 114.10, 111.01, 110.14, 44.48, 42.02, 15.21; IR (ATR) υ; 3853, 3742, 3673, 3614, 2361, 2321, 1701, 1653, 1518, 1467, 1357, 1315, 1212, 1127, 1062, 1010, 836, 796, 733, 666; HRMS (ESI^+) calculated for $C_{21}H_{17}BrN_2O_2S$ $[M+H]^+$, 441.0272; found 441.0231.

(Z)-5-((1-Benzyl-1H-indol-3-yl)methylene)-3-(4-bromobenzyl)thiazolidine-2,4-dione (6r)

Yield: 65%; Buff yellow solid; m.p: 240-241 °C; ^{1}H NMR (400 MHz, $CDCl_3$) δ 8.28 (s, 1H, -H of methylene), 7.92 – 7.82 (m, 1H, aromatic), 7.51 – 7.42 (m, 3H, aromatic), 7.34 (ddt, *J* = 13.6, 7.0, 2.3 Hz, 8H, aromatic), 7.17 (dd, *J* = 7.4, 2.0 Hz, 2H, aromatic), 5.41 (s, 2H,-CH_2), 4.87 (s, 2H,-CH_2); ^{13}C NMR (100 MHz, $CDCl_3$) δ 167.43, 166.06, 136.56, 135.57, 134.48, 132.01, 131.84, 130.63, 129.09, 128.32, 128.11, 126.97, 126.09, 123.87, 122.27, 121.95, 118.98, 114.84, 111.45, 110.60, 51.02, 44.49; IR (ATR) υ; 3852, 3742, 3673, 3614, 3107, 3019, 2360, 2325, 1671, 1520, 1470, 1373, 1335, 1188, 1144, 1017, 975, 796, 735 cm^{-1}; HRMS (ESI^+) calculated for $C_{26}H_{19}BrN_2O_2S$ $[M+H]^+$, 503.0429; found 503.0372.

(Z)-3-(4-Bromobenzyl)-5-((1-(4-chlorobenzyl)-1H-indol-3-yl)methylene)thiazolidine-2,4-dione (6s)

Yield: 53%; Buff yellow solid; m.p: 230-231 °C; ^{1}H NMR (400 MHz, $CDCl_3$) δ 8.27 (s, 1H, -H of methylene), 7.87 (ddd, *J* = 7.0, 3.3, 2.1 Hz, 1H, H_7 of indole), 7.51 – 7.41 (m, 3H, aromatic), 7.38 – 7.29 (m, 7H, aromatic), 7.13 – 7.06 (m, 2H, aromatic), 5.39 (s, 2H,-CH_2), 4.87 (s, 2H,-CH_2); ^{13}C NMR (100 MHz, $CDCl_3$) δ 167.30, 166.01, 136.38, 134.44, 134.23, 134.15, 131.85, 130.64, 130.38, 129.30, 128.18, 128.13, 125.87, 124.02, 122.31,

122.06, 119.09, 115.23, 111.70, 110.47, 50.39, 44.53; IR (ATR) υ; 3855, 3742, 3674, 3614, 2358, 1715, 1663, 1591, 1516, 1324, 1247, 1185, 1140, 1097, 1012, 976, 931, 804, 735, 664 cm^{-1}; HRMS (ESI^+) calculated for $C_{26}H_{18}BrClN_2O_2S$ $[M+H]^+$, 537.0039; found 536.9985.

(Z)-3-(4-Bromobenzyl)-5-((1-(4-bromobenzyl)-1H-indol-3-yl)methylene) thiazolidine-2,4-dione (6t)

Yield: 55%; Buff yellow solid; m.p: 240-241 °C; ^1H NMR (400 MHz, $CDCl_3$) δ 8.27 (s, 1H, -H of methylene), 7.87 (ddt, *J* = 7.0, 4.2, 2.1 Hz, 1H, H_7 of indole), 7.51 – 7.29 (m, 10H, aromatic), 7.07 – 6.97 (m, 2H, aromatic), 5.37 (s, 2H,-CH_2), 4.87 (s, 2H,-CH_2); ^{13}C NMR (100 MHz, $CDCl_3$) δ 167.29, 166.01, 136.37, 134.68, 134.44, 132.25, 131.85, 130.64, 130.38, 128.46, 128.12, 125.86, 124.03, 122.31, 122.28, 122.07, 119.10, 115.26, 111.72, 110.47, 50.45, 44.53; IR (ATR) υ; 3839, 3747, 3649, 3854, 2352, 1717, 1662, 1592, 1515, 1473, 1321, 1247, 1183, 1139, 1009, 976, 932, 800, 735, 666 cm^{-1}; HRMS (ESI^+) calculated for $C_{26}H_{18}Br_2N_2O_2S$ $[M+H]^+$, 580.9534; found 580.9493.

(Z)-3-(4-Bromobenzyl)-5-((1-(4-nitrobenzyl)-1H-indol-3-yl)methylene) thiazolidine-2,4-dione (6u)

Yield: 52%; Buff yellow solid; m.p: 241-242 °C; ^1H NMR (400 MHz, $CDCl_3$) δ 8.28 (s, 1H, -H of methylene), 8.23 – 8.15 (m, 2H, aromatic), 7.95 – 7.86 (m, 1H, aromatic), 7.54 – 7.44 (m, 3H, aromatic), 7.39 – 7.30 (m, 5H, aromatic), 7.27 – 7.20 (m, 2H, aromatic), 5.55 (s, 2H,-CH_2), 4.88 (s, 2H,-CH_2); ^{13}C NMR (100 MHz, $CDCl_3$) δ 167.12, 165.96, 147.83, 142.98, 136.24, 134.36, 131.87, 130.66, 130.16, 128.13, 127.33, 125.54, 124.36, 124.33, 122.36, 122.30, 119.31, 115.92, 112.20, 110.22, 50.30, 44.59; IR (ATR) υ; 3715, 3522, 3347, 2349, 1723, 1664, 1602, 1520, 1471, 1379, 1333, 1182, 1143, 1099, 1014, 964, 847, 797, 733, 664 cm^{-1}; HRMS (ESI^+) calculated for $C_{26}H_{18}BrN3O4S$ $[M+H]^+$, 548.0280; found 548.0209.

(Z)-5-((1H-Indol-3-yl)methylene)-3-(4-nitrobenzyl)thiazolidine-2,4-dione (6v)

Yield: 40%; Buff yellow solid; m.p: 265-266 °C; ^1H NMR (400 MHz, DMSO-d_6) δ 12.24 (s, 1H, -NH), 8.28 – 8.18 (m, 3H, aromatic), 7.92 (dt, *J* = 7.6, 1.0 Hz, 1H, H_7 of indole), 7.84 (s, 1H, H_2 of indole), 7.63 – 7.57 (m, 2H, aromatic), 7.52 (dt, *J* = 8.0, 0.9 Hz, 1H, H_4 of indole), 7.24 (dddd, *J* = 22.8, 8.0, 7.0, 1.2 Hz, 2H, aromatic), 4.98 (s, 2H,-CH_2); ^{13}C NMR (100 MHz, DMSO-d_6) δ 167.62, 165.78, 147.46, 143.80, 136.72, 129.80, 129.13,

127.25, 126.96, 124.27, 123.68, 121.72, 118.88, 113.74, 112.96, 110.91, 44.36; IR (ATR) υ; 3472, 3347, 3242, 2921, 2852, 2357, 1719, 1658, 1587, 1500, 1378, 1327, 1213, 1142, 1092, 971, 935, 807, 731, 684 cm^{-1}; HRMS (ESI^+) calculated for $C_{19}H_{13}N_3O_4S$ $[M+H]^+$, 380.0705; found 380.0639.

(Z)-5-((1-Methyl-1H-indol-3-yl)methylene)-3-(4-nitrobenzyl)thiazolidine-2,4-dione (6w)

Yield: 55%; Buff yellow solid; m.p: 237-238 °C; ^1H NMR (400 MHz, $CDCl_3$) δ 8.30 (s, 1H, -H of methylene), 8.27 – 8.18 (m, 2H, aromatic), 7.86 (dt, *J* = 7.9, 1.1 Hz, 1H, H_7 of indole), 7.67 – 7.60 (m, 2H, aromatic), 7.43 – 7.30 (m, 4H, aromatic), 5.01 (s, 2H,-CH_2), 3.93 (s, 3H,-CH_3); ^{13}C NMR (100 MHz, $CDCl_3$) δ 167.44, 165.91, 147.76, 142.46, 137.02, 131.49, 129.63, 127.88, 126.77, 123.98, 123.83, 121.94, 118.84, 113.76, 110.87, 110.10, 44.27, 33.81; IR (ATR) υ; 3853, 3742, 3673, 3614, 2363, 2318, 1746, 1699, 1653, 1516, 1467, 1381, 1328, 1232, 1128, 805, 729, 655 cm^{-1}; HRMS (ESI^+) calculated for $C_{20}H_{15}N_3O_4S$ $[M+H]^+$, 394.0862; found 394.0843.

(Z)-5-((1-Ethyl-1H-indol-3-yl)methylene)-3-(4-nitrobenzyl)thiazolidine-2,4-dione (6x)

Yield: 50%; Buff yellow solid; m.p: 200-201 °C; ^1H NMR (400 MHz, $CDCl_3$) δ 8.30 (s, 1H, -H of methylene), 8.26 – 8.18 (m, 2H, aromatic), 7.89 – 7.82 (m, 1H, aromatic), 7.70 – 7.60 (m, 2H, aromatic), 7.47 – 7.29 (m, 4H, aromatic), 5.01 (s, 2H,-CH_2), 4.30 (q, *J* = 7.3 Hz, 2H,-CH_2), 1.57 (d, *J* = 7.3 Hz, 3H,-CH_3); ^{13}C NMR (100 MHz, $CDCl_3$) δ 167.45, 165.92, 147.75, 142.49, 136.08, 129.88, 129.60, 128.10, 126.85, 123.97, 123.71, 123.59, 121.90, 121.77, 118.96, 113.58, 110.96, 110.21, 44.26, 42.08, 15.22; IR (ATR) υ; 3852, 3742, 3673, 3614, 3104, 2361, 1699, 1654, 1516, 1467, 1325, 1212, 1125, 974, 933, 801, 734 cm^{-1}; HRMS (ESI^+) calculated for $C_{21}H_{17}N_3O_4S$ $[M+H]^+$, 408.1018; found 408.0941.

(Z)-5-((1-Benzyl-1H-indol-3-yl)methylene)-3-(4-nitrobenzyl)thiazolidine-2,4-dione (6y)

Yield: 56%; Buff yellow solid; m.p: 237-238 °C; ^1H NMR (400 MHz, $CDCl_3$) δ 8.31 (s, 1H, -H of methylene), 8.28 – 8.18 (m, 2H, aromatic), 7.93 – 7.83 (m, 1H, aromatic), 7.69 – 7.58 (m, 2H, aromatic), 7.45 (d, *J* = 0.6 Hz, 1H, H_4 of indole), 7.40 – 7.30 (m, 6H, aromatic), 7.22 – 7.15 (m, 2H, aromatic), 5.43 (s, 2H-CH_2), 5.01 (s, 2H, -CH_2); ^{13}C NMR (100 MHz, $CDCl_3$) δ 167.39, 165.87, 147.77, 142.42, 136.59, 135.48, 130.78, 129.58, 129.11, 128.37, 128.09, 126.99, 126.66, 126.48, 123.97, 122.07, 118.97, 114.34, 111.41, 110.65, 51.06, 44.27; IR (ATR) υ; 3852, 3742, 3673, 3614, 3112, 3015, 2359, 1917, 1840, 1743, 1694, 1519, 1465, 1377, 1334, 1141, 1096, 796, 737, 697 cm^{-1}; HRMS ($ESI^{+)}$ calculated for $C_{26}H_{19}N_3O_4S$ $[M+H]^+$, 470.1175; found 470.1090.

(Z)-5-((1-(4-Chlorobenzyl)-1H-indol-3-yl)methylene)-3-(4-nitrobenzyl) thiazolidine-2,4-dione (6z)

Yield: 51%; Buff yellow solid; m.p: 235-236 °C; ^{1}H NMR (400 MHz, $CDCl_3$) δ 8.30 (s, 1H, -H of methylene), 8.27 – 8.18 (m, 2H, aromatic), 7.88 (ddd, *J* = 6.9, 3.2, 2.1 Hz, 1H, aromatic), 7.65 – 7.60 (m, 2H, aromatic), 7.45 (d, *J* = 0.6 Hz, 1H, H_4 of indole), 7.36 – 7.29 (m, 5H, aromatic), 7.13 – 7.06 (m, 2H, aromatic), 5.40 (s, 2H, -CH_2), 5.04 – 4.99 (m, 2H, -CH_2); ^{13}C NMR (100 MHz, $CDCl_3$) δ 167.27, 165.84, 147.77, 142.37, 136.41, 134.28, 134.06, 130.53, 129.60, 129.32, 128.19, 128.10, 126.45, 124.12, 123.99, 122.18, 119.07, 114.71, 111.64, 110.53, 50.42, 44.30; IR (ATR) υ; 3852, 3743, 3674, 3614, 2361, 2321, 1918, 1840, 1664, 1602, 1518, 1472, 1388, 1340, 1154, 1101, 1015, 802, 738, 671 cm^{-1}; HRMS (ESI^+) calculated for $C_{26}H_{18}ClN_3O_4S$ 504.0785; found 504.0691.

(Z)-5-((1-(4-Bromobenzyl)-1H-indol-3-yl)methylene)-3-(4-nitrobenzyl) thiazolidine-2,4-dione (6aa)

Yield: 52%; Buff yellow solid; m.p: 228-229 °C; ^{1}H NMR (400 MHz, $CDCl_3$) δ 8.30 (s, 1H, -H of methylene), 8.22 (d, *J* = 8.3 Hz, 2H, aromatic), 7.91 – 7.84 (m, 1H, aromatic), 7.63 (d, *J* = 8.2 Hz, 2H, aromatic), 7.52 – 7.42 (m, 3H, aromatic), 7.32 (dd, *J* = 8.5, 4.4 Hz, 3H, aromatic), 7.03 (d, *J* = 8.0 Hz, 2H, aromatic), 5.38 (s, 2H, -CH_2), 5.01 (s, 2H, -CH_2); ^{13}C NMR (100 MHz, $CDCl_3$) δ 167.27, 165.84, 147.78, 142.38, 136.41, 134.61, 132.28, 130.54, 129.61, 128.48, 128.10, 126.44, 124.14, 123.99, 122.33, 122.20, 119.08, 114.75, 111.66, 110.53, 50.49, 44.31; IR (ATR) υ; 3853, 3744, 3669, 3611, 3525, 2357, 1725, 1660, 1607, 1518, 1468, 1332, 1232, 1145, 1097, 1014, 965, 806, 730, 665 cm^{-1}; HRMS (ESI^+) calculated for $C_{26}H_{18}BrN_3O_4S$ $[M+H]^+$, 547.0280; found 548.0186.

(Z)-3-(4-Nitrobenzyl)-5-((1-(4-nitrobenzyl)-1H-indol-3-yl)methylene)thiazolidine-2,4-dione (6ab)

Yield: 50%; Buff yellow solid; m.p: 257-258 °C; ^{1}H NMR (400 MHz, $CDCl_3$) δ 8.31 (s, 1H, -H of methylene), 8.27 – 8.19 (m, 4H, aromatic), 7.94 – 7.88 (m, 1H, aromatic), 7.68 – 7.60 (m, 2H, aromatic), 7.53 – 7.19 (m, 8H, aromatic), 5.56 (s, 2H, -CH_2), 5.02 (s, 2H, -CH_2); ^{13}C NMR (100 MHz, $CDCl_3$) δ 167.08, 165.78, 147.86, 147.80, 142.89, 142.28, 136.27, 130.31, 129.63, 128.10, 127.34, 126.11, 124.43, 124.38, 124.00, 122.41, 119.29, 115.43, 112.14, 110.28, 50.34, 44.35; IR (ATR) υ; 3635, 3520, 2354, 1720, 1664, 1598,

1515, 1469, 1429, 1382, 1333, 1184, 1143, 1100, 1019, 971, 851, 804, 733, 654 cm^{-1}; HRMS (ESI^+) calculated for $C_{26}H_{18}N_4O_6S$ $[M+H]^+$, 515.1025; found 515.0925.

6.3. PL inhibition assay, enzyme kinetics and structural activity relationship

The *in-vitro* PL inhibitory activity of the synthesized analogues were evaluated by a standardised assay protocol [2,5]. As summarised in **Table 6.1**, synthesized analogues displayed potential to poor PL inhibition (IC_{50} = 6.19 to 45.00 µM). Most of the analogues exhibited good (< 15 µM) to moderate (15-30 µM) activity, while few analogues displayed poor activity (> 30 µM). Analogue **6d** exhibited the most potential activity against PL, with an IC_{50} of 6.19 µM, followed by **6e** (IC_{50} = 8.96 µM).

The inhibition mode of the topmost active analogues (**6d** and **6e**) was evaluated by performing an enzyme inhibition kinetic experiment (See chapter 3). The obtained LB plots converged at its first quadrant and intersected at one point, indicating that the analogues **6d** and **6e** exhibited a competitive mode of inhibition (**Fig. 6.3**). A proportionate increase in the apparent K_m values without affecting the V_{max} further indicated reversible competitive inhibition (**Table 6.2**). Inhibition constant (K_i) values were deduced as 3.931 and 5.691 µM (retrieved from the Cheng-Prusoff equation [6]), proving that these analogues had a strong affinity towards PL. From the enzyme kinetics study, it can be concluded that the synthesized analogues were bound to the active site of the PL during the inhibition.

Table 6.1 *In-vitro* PL inhibitory activity of the synthesized analogues (6a- 6ab)

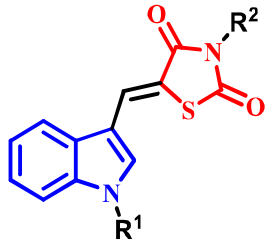

#	R^1	R^2	IC_{50} (µM) *	#	R^1	R^2	IC_{50} (µM) *
6a	H	Benzyl	23.42 ± 1.75	6o	H	4-Bromobenzyl	34.98 ± 3.83
6b	Methyl	Benzyl	14.39 ± 0.75	6p	Methyl	4-Bromobenzyl	45.00 ± 2.32
6c	Ethyl	Benzyl	10.52 ± 1.25	6q	Ethyl	4-Bromobenzyl	14.66 ± 2.29
6d	**Benzyl**	**Benzyl**	**6.19 ± 0.66**	6r	Benzyl	4-Bromobenzyl	20.06 ± 1.58
6e	**4-Chlorobenzyl**	**Benzyl**	**8.96 ± 0.80**	6s	4-Chlorobenzyl	4-Bromobenzyl	25.56 ± 2.12
6f	4-Bromobenzyl	Benzyl	13.22 ± 1.24	6t	4-Bromobenzyl	4-Bromobenzyl	25.02 ± 1.98
6g	4-Nitrobenzyl	Benzyl	18.29 ± 0.33	6u	4-Nitrobenzyl	4-Bromobenzyl	33.14 ± 0.41
6h	H	4-Chlorobenzyl	35.69 ± 3.28	6v	H	4-Nitrobenzyl	27.14 ± 2.66
6i	Methyl	4-Chlorobenzyl	23.34 ± 0.79	6w	Methyl	4-Nitrobenzyl	23.57 ± 2.00
6j	Ethyl	4-Chlorobenzyl	28.23 ± 3.93	6x	Ethyl	4-Nitrobenzyl	27.70 ± 2.01
6k	Benzyl	4-Chlorobenzyl	9.14 ± 2.42	6y	Benzyl	4-Nitrobenzyl	18.76 ± 1.15
6l	4-Bromobenzyl	4-Chlorobenzyl	23.71 ± 2.22	6z	4-Chlorobenzyl	4-Nitrobenzyl	21.36 ± 1.11
6m	4-Chlorobenzyl	4-Chlorobenzyl	22.69 ± 0.62	6aa	4-Bromobenzyl	4-Nitrobenzyl	26.56 ± 1.56
6n	4-Nitrobenzyl	4-Chlorobenzyl	31.63 ± 0.92	6ab	4-Nitrobenzyl	4-Nitrobenzyl	36.73 ± 1.59

* All the experiments were performed in triplicate and the values are represented as mean ± S.E.M

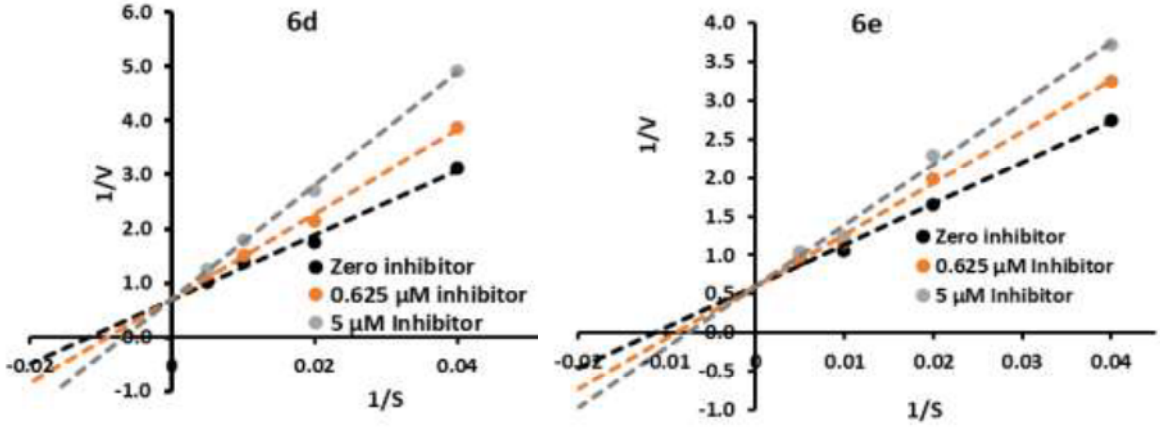

Fig. 6.3. Double reciprocal Lineweaver-Burk plots of analogues 6d and 6e

Table 6.2. K_m, V_{max} and K_i values of **6d** and **6e** retrieved from the PL enzyme kinetics

Code	K_m (apparent) at different concentration (µM)			V_{max} (µM/min)	K_i µM	Nature of inhibition
	0 µM	0.625 µM	5 µM			
6d	84.545	109.672	148.084	1.413	3.931	Competitive
6e	88.567	111.585	132.383	1.670	5.691	Competitive

Based on the *in-vitro* PL inhibition assay, a preliminary structure-activity relationship of the screened analogues has been deduced and a similar relationship has been observed with the Series I. As represented in **Fig. 6.4**, the presence of aromatic functionalities on the indole scaffold significantly increased the PL inhibition activity of analogues in comparison to the alkyl/ unsubstituted counterparts. For instance, **6d** with a benzyl substitution exhibited higher PL inhibitory activity (IC_{50} = 6.19 µM) than the unsubstituted/alkyl substitutions (**6a** to **6c** with an IC_{50} value ranges 10.52 to 23.42 µM). Further, an additional substitution on the aryl ring resulted in the variation in the PL inhibitory potential. Ring deactivating groups resulted in the weakening of the potency, wherein -NO_2 substitution resulted in the poorest activity. Previous studies (chapter 5) revealed that the simple alkyl substitutions do not impart a significant role in the PL inhibition. Hence, in the present series, aromatic functionalities have only been substituted with the TZD. Substitution of the electron-withdrawing substituents in the TZD resulted in the reduction of the PL inhibitory activity. Analogue **6k** possessing a 4-chlorobenzyl

substituent on imidic nitrogen was less active (IC_{50} = 9.14 µM) than **6d**, that lacked electron withdrawing group in the aromatic functionality (IC_{50} = 6.19 µM). Nitro substituted analogues (**6y** and **6ab**) exhibited the comparatively lesser activity (IC_{50} = 18.76 and 36.73 µM, respectively) than the -Cl substituted analogues (**6k** and **6n**; IC_{50} = 9.14 and 31.63 µM, respectively). Based on these observations, a preliminary structural activity relationship was deduced and represented in **Fig. 6.4.**

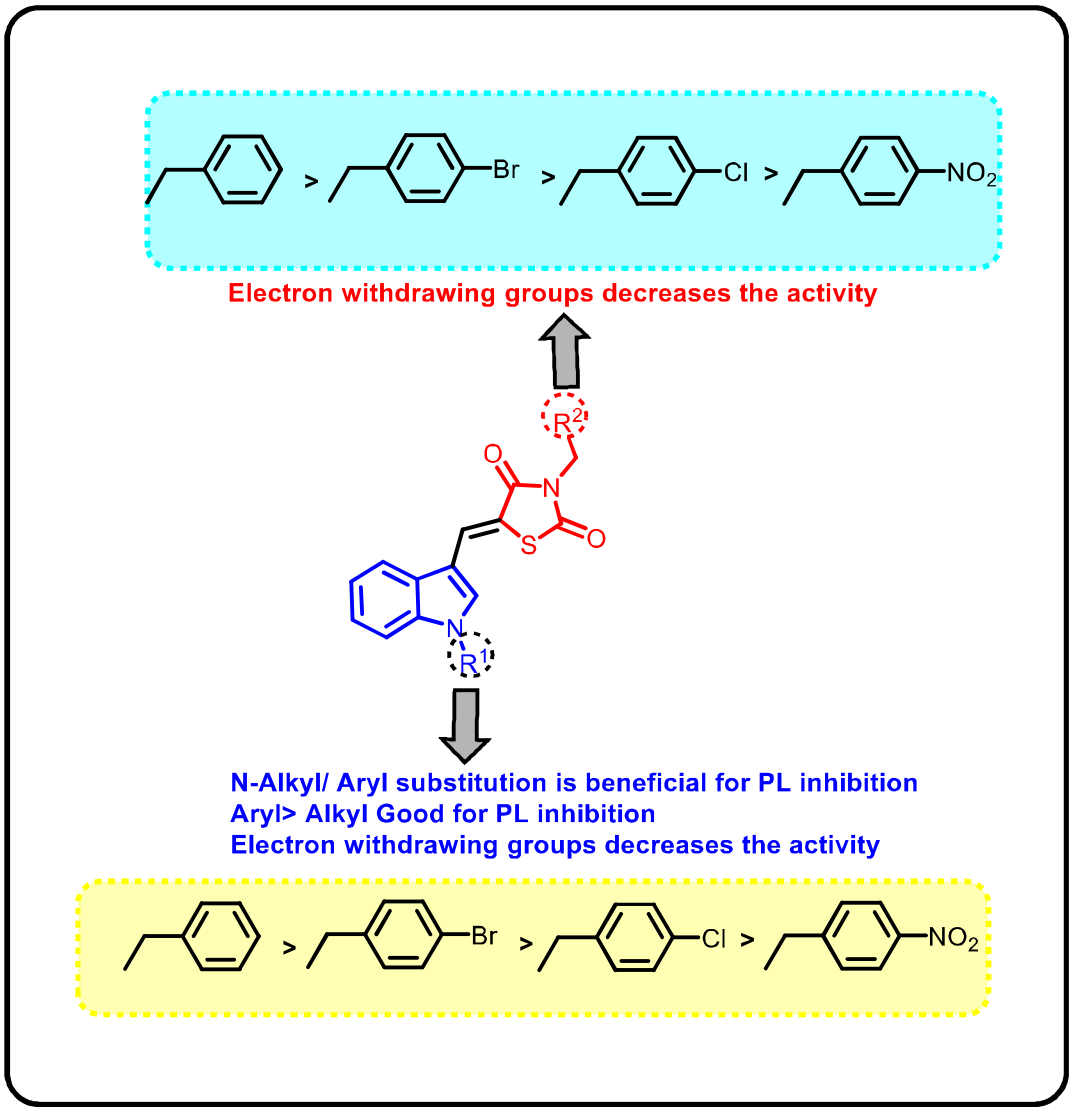

Fig. 6.4. Structure-activity relationship of synthesized Indole-TZD hybrid analogues (**6a-6ab**)

6.4. Fluorescence Quenching Measurements with PL

The effects of the synthesized analogues (**6d** and **6e**) in the fluorescence quenching of PL were evaluated (See chapter 5) and the results are depicted in **Fig. 6.5** and **Table 6.3**. The screened analogues exerted a concentration dependant quenching effect to the PL fluorescence.

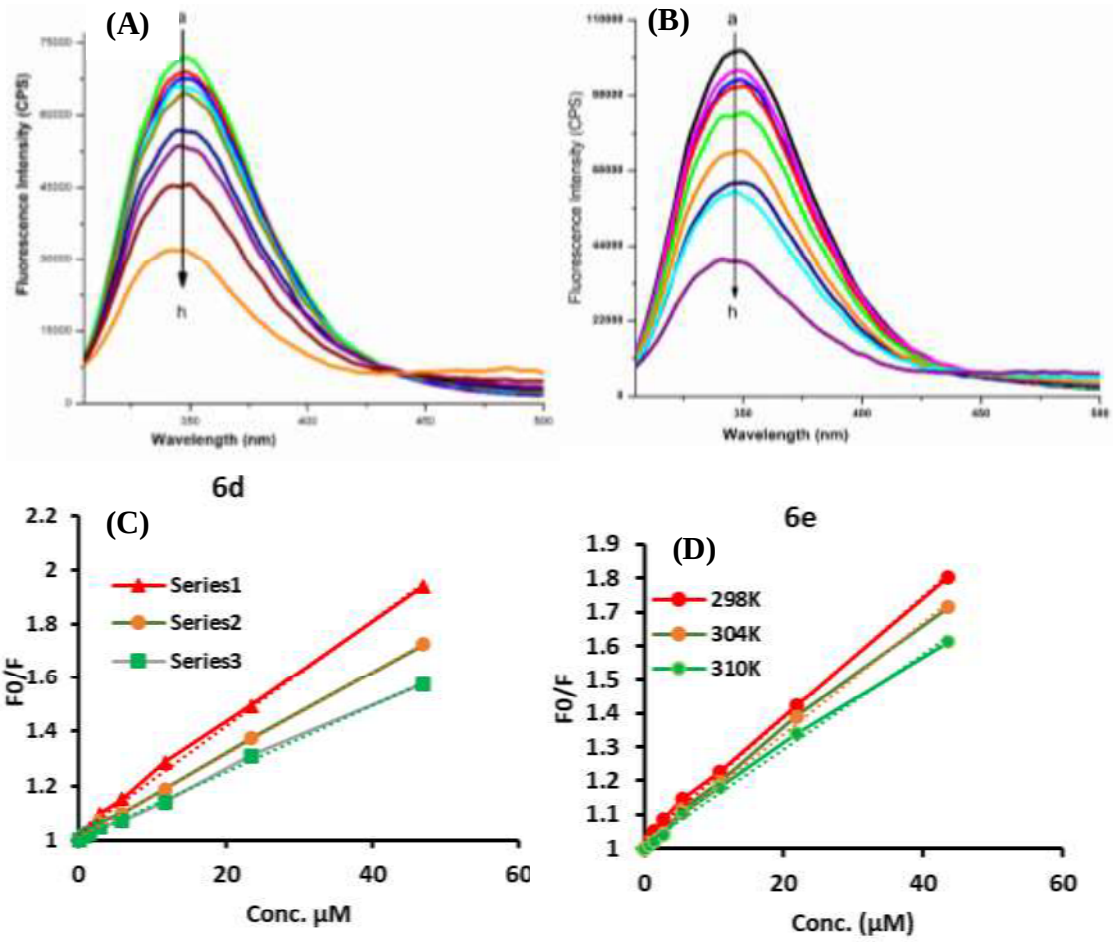

Fig. 6.5. (A), (B) The fluorescence spectra of PL in the presence of **6d** and **6e** at various concentrations (pH 7.4, a to h in increasing concentrations); (C), (D) Stern−Volmer plots for the quenching of **6d** and **6e** on the PL at 300K

As represented in **Table 6.3**, an inverse correlation between the K_{sv} and temperature was obtained, that suggested the quenching effects on the PL may be mainly attributed to static quenching. Furthermore, K_q values were in the range of 77 to 125 (10^{10} M^{-1} s^{-1}) supporting the static mechanism-based quenching wherein both analogues formed a complexes with PL.

Based on the modified Stern-Volmer equation, the number of binding sites and binding constant were calculated, that further supported the inhibitory potential of these analogues. The values of "*n*" at the corresponding temperature were in the range of 0.808 to 1.048 indicating that these analogues bind to the active site. This fact further supported the competitive inhibition deduced from the enzyme inhibition kinetics. Moreover, a strong binding force of these analogues with PL was identified from the strong binding constants (K_b), that were in the range 1.37 to 3.32 ($\times 10^4$ M^{-1} s^{-1})

Table 6.3. Bimolecular quenching constant (K_q), binding constant (K_b) and the number of binding sites (n) at different temperatures for **6d** and **6e**

#	T (K)	K_{SV} ($\times 10^4$ M^{-1})	K_q ($\times 10^{10}$ M^{-1} s^{-1})	R^2	K_b ($\times 10^4$ M^{-1} s^{-1})	n	R^2
	298	1.98	124.53	0.9893	3.32	0.836	0.9882
6d	304	1.53	96.23	0.999	2.19	0.899	0.9948
	310	1.23	77.36	0.9978	1.74	0.892	0.9938
	298	1.80	113.21	0.9971	3.60	0.808	0.9970
6e	304	1.65	103.77	0.9970	2.05	0.940	0.9870
	310	1.42	89.31	0.9951	1.37	1.048	0.9918

6.5. Molecular docking and Dynamics

A total of 28 indole-TZD hybrid analogues were subjected to molecular docking studies, while the most active analogues **6d** and **6e** were also subjected to MD simulations. The MolDock scores and the various interactions exhibited by the hybrid analogues are summarized in **Table 6.4** and **Fig. 6.6**. The MolDock scores of the analogues exhibited significant correlation to their PL inhibitory activity (Pearson's $r = 0.8682$, $p < 0.05$) and these activities were exerted *via* various interactions such as hydrogen bonding, π- π stacking, π-sulfur and π-cation etc. The most active analogue (**6d)** from the series possessed a top docking score of -115.619 kcal/mol, while **6e**, the second most active in the series, exhibited a MolDock score of -108.706 kcal/mol. Majority of the analogues exhibited consistent H-bond interactions with Gly76, Phe77, His 151 and Ser152. Since the current series mainly relied on the aromatic substitutions over the simple alkyl substitution in the imidic nitrogen atom, prominent π-π interactions were observed with the lid domain amino acid (Phe 77, Phe 215). An π-sulfur interaction has been observed with the catalytic triad amino acid, His 263. Numerous π-alkyl and π-cation interactions were also obtained during the molecular docking studies (**Table 6.4**).

Table 6.4. Mol Dock scores (in kcal/ mol) and the interaction summary of the synthesized analogues **(6a- 6ab)** with the human PL active site of 1LPB

#	Mol Dock Score	H-bond	π-π interaction	π-cation	Alkyl/π-alkyl	π-Sulfur
6a	-82.373	His-151, Ser-152	Phe-77, Phe-215	Asp-79, His-151, Arg-256, His-263	Ile-78, Ala-178	His-263
6b	-99.781	Gly-76, Phe-77, His-151	Phe-77	Asp-79, His-151, Arg-256, His-263	Ile-78, Ala-178, Pro-180, Leu-264	His-263
6c	-102.054	Gly-76, Phe-77, His-151	Phe-77	His-151, His-263	Tyr-114, Pro-180, Ile-209, Phe-215, Ala-259, Ala-260, Leu-264,	His-263
6d	-115.619	Gly-76, Phe-77, His-151	Phe-77, Phe-215	Asp-79, His-151, Arg-256, His-263	Ile-78, Ala-178, Pro-180, Ala-259, Ala-260, Leu-264	His-263
6e	-108.706	His-151, Ser-152	Phe-77, Tyr-114	Asp-79, His-151, Arg-256, His-263	Ile-78, Ala-178, Pro-180	His-263
6f	-97.120	Gly-76, Phe-77, His-151	Phe-77	Asp-79, His-151, Arg-256, His-263	Ile-78, Ala-178, Pro-180, Ala-259, Ala-260, Leu-264	His-263
6g	-88.201	Gly-76, Phe-77, His-151	Phe-77, Tyr-114	His-151, His-263	Ala-259, Ala-260, Leu-264	His-263
6h	-75.769	His-151, Ser-152	Phe-77, Phe-215	Asp-79, His-151, Arg-256, His-263	Ile-78, Ala-178, Trp-252	His-263
6i	-89.261	Gly-76, Phe-77, His-151	Phe-77	Asp-79, His-151, Arg-256, His-263	Ile-78, Ala-178, Pro-180, Trp-252, Leu-264	His-263
6j	-85.731	Gly-76, Phe-77, His-151	Phe-77	Asp-79, His-151, Arg-256, His-263	Ile-78, Pro-180, Ile-209, Phe-215, Trp-252, Leu-264	His-263
6k	-105.369	Gly-76, Phe-77, His-151	Phe-77, Tyr-114	Asp-79, His-151, Arg-256, His-263	Ile-78, Ala-178, Pro-180, Ala-259, Ala-260, Leu-264	His-263

…. Contd

#	Mol Dock Score	H-bond	π-π interaction	π-cation	Alkyl/π-alkyl	π-Sulfur
6l	-90.893	Gly-76, Phe-77, His-151	Phe-77	Asp-79, His-151, Arg-256, His-263	Ile-78, Ala-178, Pro-180, Ala-259, Ala-260, Leu-264	His-263
6m	-91.883	Gly-76, Phe-77, His-151	Phe-77	Asp-79, His-151, Arg-256, His-263	Ile-78, Ala-178, Pro-180, Ala-259, Ala-260, Leu-264	His-263
6n	-82.606	--	Phe-77, Tyr-114	His-151, His-263	Ala-178, Pro-180, Ile-209, Phe-215	Tyr-114
6o	-85.420	His-151, Ser-152	Phe-77, Phe-215	Asp-79, His-151, Arg-256, His-263	Ile-78, Ala-178, Trp-252	His-263
6p	-72.392	Gly-76, Phe-77, His-151	Phe-77	Asp-79, His-151, Arg-256, His-263	Ile-78, Trp-252, Leu-264	His-263
6q	-89.606	Gly-76, Phe-77, His-151	Phe-77	Asp-79, His-151, Arg-256, His-263	Ile-78, Pro-180, Ile-209, Phe-215, Trp-252, Leu-264	His-263
6r	-92.304	His-151, Ser-152	Phe-77, Tyr-114	Asp-79, His-151, Arg-256, His-263	Ile-78, Ala-178, Pro-180, Trp-252, Leu-264	His-263
6s	-85.671	Gly-76, Phe-77, His-151	Phe-77, Tyr-114	Asp-79, His-151, Arg-256, His-263	Ile-78, Leu-264	His-263
6t	-91.267	Gly-76, Phe-77, His-151	Phe-77	Asp-79, His-151, Arg-256, His-263	Ile-78, Ala-178, Pro-180, Ala-260, Leu-264	His-263

…. Contd

#	Mol Dock Score	H-bond	π-π interaction	π-cation	Alkyl/π-alkyl	π-Sulfur
6u	-89.586	Arg-256	Phe-77, Phe-215	Asp-79, His-151, His-263	Ala-259, Ala-260, Leu-264	--
6v	-94.412	His-151, Ser-152, Arg-256	Phe-77, Phe-215	Asp-79, His-151, Arg-256, His-263	Ile-78, Ala-178, Leu-264	His-263
6w	-91.754	Gly-76, Phe-77, His-151, Arg-256	Phe-77, Tyr-114	Asp-79, His-151, Arg-256, His-263	Ile-78, Ala-178, Pro-180, Leu-264	His-263
6x	-97.880	Gly-76, Phe-77, His-151, Arg-256	Phe-77	Asp-79, His-151, Arg-256, His-263	Ile-78, Tyr-114, Pro-180, Ile-209, Phe-215, Leu-264	His-263
6y	-93.717	Gly-76, Phe-77, His-151	Phe-77, Tyr-114	His-151, His-263	Ala-259, Ala-260, Leu-264	His-263
6z	-86.451	Gly-76, Phe-77, His-151	Phe-77, Tyr-114	His-151, His-263	Ala-259, Ala-260, Leu-264	His-263
6aa	-85.598	Gly-76, Phe-77, His-151, Arg-256	Phe-77	His-151, Arg-256, His-263	Ile-78, Leu-264	His-263
6ab	-83.6430	His-151, Ser-152, Arg-256	Phe-77, Tyr-114, Phe-215	Asp-79, His-151, Arg-256, His-263	Ile-78, Ala-178, Pro-180, Ile-209, Leu-264	His-263
Orlistat	-107.750	Phe-77, Ser 152, His 263	Tyr-114, Trp-252	--	Arg-256, Ala-259,	--

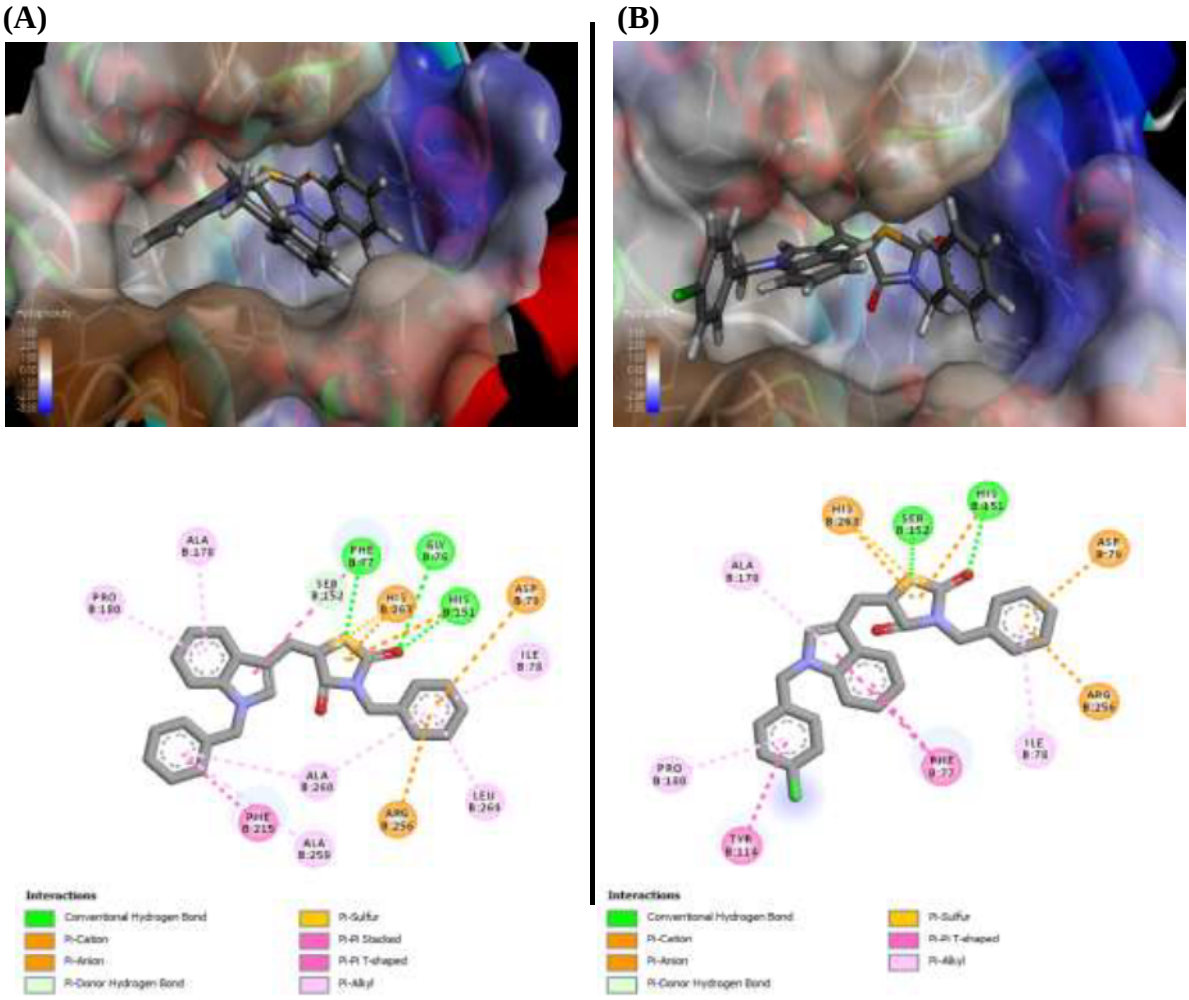

Various interactions of the analogues with PL (1LPB) were identified by using the molecular modelling studies. Further, a 20 ns MD simulation were performed for **6d** and **6e**, that provided information about the stability of the binding mode and interactions in a dynamic environment. Both the analogues (**6d** and **6e**) exhibited a stable binding conformation throughout the simulation (**Fig. 6.7**). Analogues **6d** and **6e** exhibited a maximum deviation of ≈ 0.8 nm (at ≈10 ns) and ≈ 0.5 nm (at ≈ 7.5 ns), respectively. Furthermore, a stable radius of gyration indicated the compactness of the 1LPB during the MD run with these analogues.

The obtained interactions during the course of 20 ns MD simulation of these analogues with 1LPB complex are summarised in **Table 6.5.** The analogues exhibited numerous interactions such as H bonding, π-π interaction, π-alkyl and π-sulfur interactions etc.

Fig.

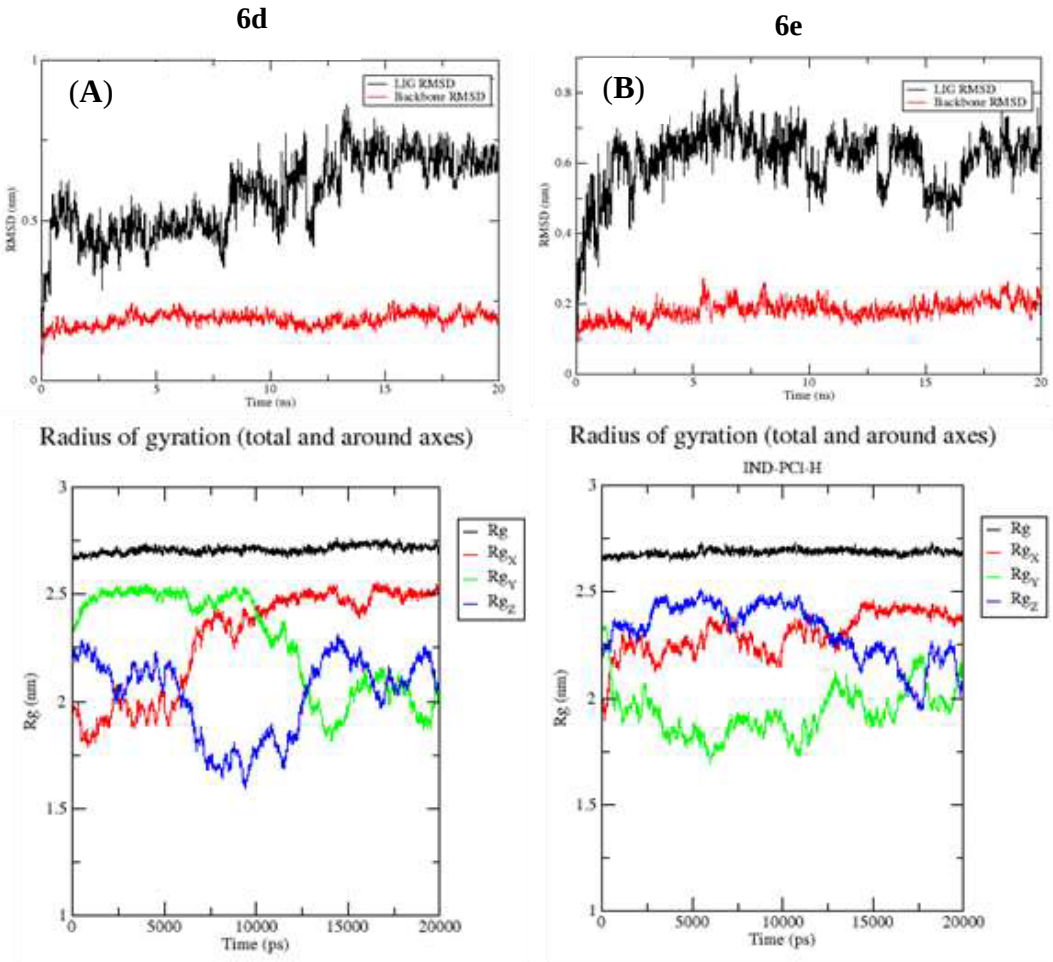

6.7. RMSD of Ligands and Radius of gyrations retrieved from 20 ns MD simulations of the PL-ligand complex (A)- **6d**; (B)- **6e**.

In case of **6d**, initially, H bond interaction was formed with the Ser 152 whereas prominent π-π interactions with lid domain amino acids (Phe 77, Tyr 114 and Phe 215) were observed throughout the simulation. Apart from these, π-sulfur interactions were also exhibited with lid domain and catalytic triad amino acids.

In case of **6e**, H bond was formed with the Ser 152 during the later stages of the simulations, whereas π-π interactions were prominent during the entire tenure. Numerous π-alkyl interactions were observed, wherein various amino acids such as Ile 78, Pro 180, Arg 256, Ala 259, Ala 260, Leu 264 etc. were involved. Additionally, **6e** exerted π-sulfur interaction with Phe 77, Tyr 114, His-151, Phe 215 and His-263.

Table 6.5. Various interactions exhibited by **6d** and **6e** during the 20 ns MD run

Time (ns)	H Bond	π-π Interaction	π -alkyl	π -Sulfur
6d				
0	--	Phe-77, Tyr-114, Arg-256, His-263	Ile-78, Ala-259	His-151, His-263
2	Ser-152	Phe-215, His-263	Ala-260	--
4	Ser-152	His-263	Ala-260	--
6	Ser-152	Phe-77, Phe-215, His-263	Leu-213, Ala-260	Phe-77, Phe-215
8	Ser-152	Phe-77	Ile-78, Ala-260	Phe-77
10	--	Phe-215, His-263	Ala-260	Phe-77
12	--	Phe-77, Phe-215	Leu-213, Ala-260	--
14	--	Phe-77, Tyr-114	--	--
16	--	Thr-112, Tyr-114, Phe-215	Ile-209	--
18	--	Tyr-114, Phe-215	Ile-78, Ile-209	Phe-215
20	--	Tyr-114, Phe-215	Pro-180, Leu-213	--
6e				
0	--	Phe-77	Ile-78, Pro-180, Ala-259	His-151, His-263
2	--	Phe-77, Tyr-114	Ile-78, Pro-180, Ala-259, Arg-256, Ala-260, Leu-264	Phe-77, His-263
4	--	Phe-77	Ile-78, Arg-256, Ala-260	Phe-215
6	--	Phe-77, Tyr-114	Ile-78, Arg-256, Ala-259, Ala-260	Phe-77, His-263
8	--	Phe-77	Ile-78, Ala-259, Ala-260, Leu-264	Phe-77
10	Ser-152	Phe-77, Phe-215	Ile-78, Ala-259, Leu-264	Phe-77
12	Ser-152	Phe-77, Phe-215	Ile-78, Ala-259, Ala-260, Leu-264	Phe-77, Tyr-114
14	Ser-152	Phe-77	Ile-78, Ala-259, Leu-264	Phe-77, Tyr-114
16	Ser-152	--	Ile-78, Ala-259, Leu-264	Phe-77
18	Ser-152	Phe-77, Tyr-114, Phe-215	Ile-78	--
20	--	--	Ala-259, Ala-260	Phe-215

In conclusion, the chapter was aimed to reduce the interaction distance between the reactive functionalities and Ser 152. Incorporation of a carbon linker between the indole and TZD resulted in the reduction of the interaction distance. Based on these observations, a series of indole-TZD hybrid analogues (**6a** to **6ab**) were synthesized and evaluated for their *in-vitro* PL inhibition activity. Among the synthesized analogues, **6d** was found to be the most active inhibitor of PL with an IC_{50} of 6.19 µM, followed by **6e** (IC_{50} = 8.96 µM). A competitive mode of enzyme inhibition was exerted by these analogues and these facts were correlated to the fluorescence quenching studies, wherein the presence of one binding site was confirmed. Moreover, molecular modelling studies (Molecular docking and dynamics) validated the rationale for the structural modification of the hybrid analogues.

Though the synthesized analogues exhibited a potential PL inhibition than the Series I, improvement in PL inhibition was thought to be obtained from further structural modifications. This is discussed in the next chapter.

References

[1] S.N.C. Sridhar, S. Palawat, A.T. Paul, Design, synthesis, biological evaluation and molecular modelling studies of conophylline inspired novel indolyl oxoacetamides as potent pancreatic lipase inhibitors, New J. Chem. 44 (2020) 12355–12369.

[2] S.N.C. Sridhar, D. Bhurta, D. Kantiwal, G. George, V. Monga, A.T. Paul, Design, synthesis, biological evaluation and molecular modelling studies of novel diaryl substituted pyrazolyl thiazolidinediones as potent pancreatic lipase inhibitors, Bioorg. Med. Chem. Lett. 27 (2017) 3749–3754.

[3] K. Tilekar, N. Upadhyay, N. Jänsch, M. Schweipert, P. Mrowka, F.J. Meyer-Almes, C.S. Ramaa, Discovery of 5-naphthylidene-2,4-thiazolidinedione derivatives as selective HDAC8 inhibitors and evaluation of their cytotoxic effects in leukemic cell lines, Bioorg. Chem. 95 (2020) 103522.

[4] Y. Momose, K. Meguro, H. Ikeda, C. HatanakaA, S. Oi, T. Sohda, Studies on Antidiabetic Agents. X. Synthesis and Biological Activities of Pioglitazone and Related Compounds., Chem. Pharm. Bull. (Tokyo). 39 (1991) 1440–1445.

[5] G. George, P.S. Dileep, A.T. Paul, Development and validation of a new HPTLC-HRMS method for the quantification of a potent pancreatic lipase inhibitory lead Echitamine from *Alstonia scholaris*, Nat. Prod. Res. (2019) 1–5.

[6] B.T. Burlingham, T.S. Widlanski, An intuitive look at the relationship of K_i and IC_{50}: A more general use for the Dixon plot, J. Chem. Educ. 80 (2003) 214-217.